EurJOC
European Journal of Organic Chemistry

A Journal of
ChemPubSoc Europe

Accepted Article

Title: Synthesis and characterization of hairpin mimics that modulate amyloid beta-peptide early oligomerization and fibrillization

Authors: Umberto Piarulli, Leila Vahdati, Julia Kaffy, Dimitri Brinet, Guillaume Bernadat, Isabelle Correia, Silvia Panzeri, Roberto Fanelli, Olivier Lequin, Miriam Taverna, and Sandrine Ongeri

To be cited as: *Eur. J. Org. Chem.* 10.1002/ejoc.201700010

Link to VoR: http://dx.doi.org/10.1002/ejoc.201700010

Supported by
ACES Asian Chemical Editorial Society

WILEY-VCH

10.1002/ejoc.201700010

WILEY-VCH

FULL PAPER

Hairpins hold it firmly The small hairpin mimic containing a cis-diketopiperazine scaffold as a turn inducer, is able to decrease the aggregation of amyloid peptide Aβ1-42 and prevent the formation of oligomeric and neurotoxic species.

.

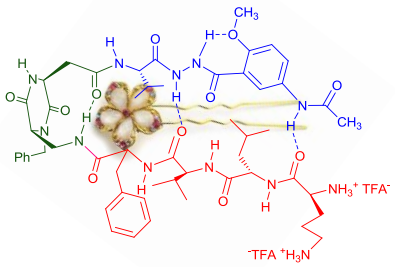

Amyloid-Oligomerization Modulators

Leila Vahdati, Julia Kaffy, Dimitri Brinet, Guillaume Bernadat, Isabelle Correia, Silvia Panzeri, Roberto Fanelli, Olivier Lequin, Myriam Taverna, Sandrine Ongeri, and Umberto Piarulli**

Page No. – Page No.

Synthesis and characterization of hairpin mimics that modulate amyloid β-peptide early oligomerization and fibrillization

10.1002/ejoc.201700010

WILEY-VCH

Synthesis and characterization of hairpin mimics that modulate amyloid β-peptide early oligomerization and fibrillization

Leila Vahdati,[a,b] Julia Kaffy,[b] Dimitri Brinet,[b,c] Guillaume Bernadat,[b] Isabelle Correia,[d] Silvia Panzeri,[a] Roberto Fanelli,[a] Olivier Lequin,[d] Myriam Taverna,[c] Sandrine Ongeri,*[b] and Umberto Piarulli*[a]

Dedicated to Professor Cesare Gennari on the occasion of his 65th birthday

Abstract: Alzheimer's disease is a neurodegenerative disorder linked to oligomerization and fibrillization of different amyloid β peptide isoforms. Among these amyloid peptides, $A\beta_{1-42}$ is considered as the most aggregative and neurotoxic species. We report herein the synthesis of four β-sheet mimics composed of a peptidomimetic arm based on a 5-amino-2-methoxy benzhydrazide derivative, a 2,5-diketopiperazine scaffold (either *cis*-DKP or *trans*-DKP) and a tetrapeptide sequence (either Gly-Val-Val-Ile, GVVI, or Lys-Leu-Val-Phe, KLVF). The derivatives containing the *cis*-DKP were shown by NMR and computational studies to adopt a stable β-hairpin conformation in solution, whereas the *trans*-DKP scaffold promoted the formation of extended structures. The activity of these compounds in modulating the aggregation of $A\beta_{1-42}$ peptide was investigated by Thioflavin T fluorescence assay to measure the kinetics of aggregation. Capillary electrophoresis (CE) and transmission electron microscopy (TEM) were then used to monitor the formation of small soluble Aβ oligomers and higher molecular weight and insoluble Aβ aggregates, respectively. As a result, small hairpin mimics containing the *cis*-DKP scaffold are able to prevent the formation of small $A\beta_{1-42}$ oligomeric and neurotoxic species.

Introduction

The role of protein-protein interactions in protein aggregation has been extensively investigated, suggesting that cumulative protein misfolding in the aggregation process (i.e. amyloidogenesis) can be associated to more than 20 serious human diseases and can play a leading role in neurodegenerative diseases, such as Alzheimer's disease (AD), Parkinson's disease (PD), as well as other systemic disorders characterized by the accumulation of insoluble protein deposits (e.g. type II diabetes mellitus).[1] AD, which is the most common form of late-life dementia,[2] is associated with the accumulation of intraneuronal neurofibrillary tangles composed of paired helical filaments of hyperphosphorylated tau protein and extracellular plaques containing insoluble fibrils made of 40 or 42-residue amyloid β–peptides ($A\beta_{1-40}$ or $A\beta_{1-42}$).[3] $A\beta_{1-42}$ is the predominant form in amyloid plaques and is by far more aggregative and neurotoxic than $A\beta_{1-40}$.[4,5] The conversion of monomeric Aβ peptides into fibrils proceeds through a complex nucleation process and involves the formation of various aggregated species such as soluble oligomers and protofibrils of increasing size,[6,7,8] which are structured in β-sheet-rich conformations involving the hydrophobic central ($K_{16}LVFFA_{21}$) and *C*-terminal ($I_{31}IGLMVGGVVIA_{42}$) sequences.[9,10,11,12,13] Low molecular weight oligomers have been considered for the last decade by several groups, as primarily responsible for the neurodegeneration observed in AD, by inducing physical changes in the cell membrane leading to dysfunction and cell death.[3,4,14,15,16,17] In addition, fibrils are not inert species as they have been demonstrated to generate damaging redox activity and promote the nucleation of toxic oligomers.[18] As a consequence, reducing the prevalence of both fibrils and small transient oligomers has become an essential criterion for the evaluation and selection of small therapeutic molecules. Much of the research effort aimed at targeting the aggregation process of $A\beta_{1-42}$ has been focused on retarding the fibrillogenesis, [19,20,21] and, although many compounds have been reported to inhibit the aggregation, their mechanism of action and effects on oligomers formation remain unclear to date, thus hampering their development as drug candidates.[22,23] Some peptide derivatives have also shown interesting inhibition activities on $A\beta_{1-42}$ aggregation.[24] Recently, the assumption that preorganized strands in β-hairpin mimics will promote the association and sheet formation with $A\beta_{1-42}$ thus preventing, or at least delaying its aggregation, has been validated by macrocyclic β-sheet mimic structures.[25,26,] However, to our knowledge, only rare examples of acyclic β-hairpins have been demonstrated as $A\beta_{1-42}$ binders and inhibitors of aggregation. [27,28,29,30]. On the other hand, the exclusive or very high peptidic character of these compounds would definitely hamper their development as drugs. We hypothesized that maintaining an acyclic β-hairpin while decreasing the peptidic character could provide valuable insights to develop β-hairpin mimics with higher drug-like characteristics. For that purpose, we describe the

[a] Dr. L.Vahdati, Dr S. Panzeri, Dr. R. Fanelli, Prof. Dr. U. Piarulli
Università degli Studi dell'Insubria
Dipartimento di Scienza e Alta Tecnologia
Via Valleggio 11, 22100 Como (Italy)
E-mail: umberto.piarulli@uninsubria.it
Url: http://www4.uninsubria.it/on-line/home/rubrica/home-page-personale.html?P1_m=P000228

[b] Dr. J. Kaffy, Dr. D. Brinet, Dr. G. Bernadat, Prof. Dr. S. Ongeri
BioCIS, Univ. Paris-Sud, CNRS, Université Paris-Saclay, 92290, Châtenay-Malabry, FRANCE
E-mail: Sandrine.ongeri@u-psud.fr

[c] Dr. D. Brinet, Prof. Dr. M. Taverna
Protéins and Nanotechnology in analytical science, Institut Galien de Paris Sud, Univ. Paris-Sud, CNRS, Université Paris-Saclay, 92290, Châtenay-Malabry, FRANCE

[d] Dr. I. Correia, Prof. Dr. O. Lequin
Sorbonne Universités, UPMC Univ Paris 06, Ecole Normale Supérieure, PSL Research University, CNRS, Laboratoire des Biomolécules, 4 place Jussieu, 75252 Paris Cedex 05, France

Supporting information for this article is given via a link at the end of the document.((Please delete this text if not appropriate))

synthesis of a new class of peptidomimetics (Figure 1), containing a bifunctional diketopiperazine scaffold DKP, as a potential β-turn inducer, a peptidomimetic arm and a tetrapeptide arm. As peptidomimetic arm, we inserted the 5-amino-2-methoxybenzhydrazide unit, which is a part of the β-strand mimic ("Hao" unit) used by Nowick and co-workers.[26] The four amino acid residues were selected from hydrophobic $A\beta_{1-42}$ sequences playing a crucial role in the β-sheet structuration of $A\beta_{1-42}$ aggregates. The bifunctional diketopiperazines introduced in these constructs, were recently developed in our group as effective inducers of the secondary protein structure. In fact, short peptidic sequences containing the *cis*-DKP scaffold (Figure 1), were shown by NMR and molecular modeling studies to adopt very stable β-hairpin structures,[31] whereas the *trans*-DKP scaffold effectively induced β-turn conformations in short cyclic peptides.[32] The activity of these compounds in modulating $A\beta_{1-42}$ early oligomerization and fibrillization was finally investigated using a combination of different assays: thioflavin T fluorescence assay, capillary electrophoresis (CE) and transmission electron microscopy (TEM).

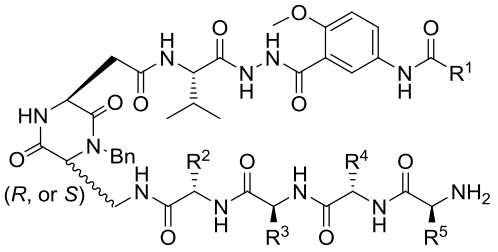

1, (*S*), R^1= CH_3, R^2= *s*Bu, R^3= *i*Pr, R^4= *i*Pr, R^5= H
2, (*S*), R^1= CF_3, R^2= CH_2Ph, R^3= *i*Pr, R^4= *i*Bu, R^5=$(CH_2)_4NH_2$
3, (*R*), R^1= CH_3, R^2= *s*Bu, R^3= *i*Pr, R^4= *i*Pr, R^5= H
4, (*R*), R^1= CF_3, R^2= *s*Bu, R^3= *i*Pr, R^4= *i*Pr, R^5= H

Figure 1. Structure of compounds **1-4** containing a *cis* or *trans* diketopiperazine scaffold, a peptidomimetic arm and a peptidic arm

Results and Discussion

Synthesis and characterization of peptidomimetics 1-4

To establish a relationship between the structure of these peptidomimetics with respect to the affinity towards $A\beta_{1-42}$, several structural elements of these compounds were taken into consideration: 1) the importance of the β-hairpin structure: *cis* versus *trans*-DKP scaffold, the presence of two arms linked to the scaffold versus only one arm, the activity of the isolated tetrapeptide and peptidomimetic arms; 2) the hydrophobic peptidic sequence: Gly-Val-Val-Ile versus Lys-Leu-Val-Phe, that are part of the *C*-terminal ($G_{38}VVI_{41}$) and the central ($K_{16}LVF_{19}$) $A\beta_{1-42}$ sequences respectively, both involved in stabilizing $A\beta_{1-42}$ aggregates;[9-13] 3) the effect of introducing a hydrophobic trifluoromethyl group versus a methyl group; and 4) the possibility of forming electrostatic interactions with acidic residues of $A\beta_{1-42}$, by cleaving the *N*-protecting groups in all the final products. In this way the structures of compounds **1-4** were devised.

Compound **1,** containing the *cis*-DKP linked to the tetrapeptide GVVI and a peptidomimetic arm was recently prepared[33] according to Scheme 1, which was also followed for the synthesis of the remaining derivatives **2**-**4**: Boc-5-amino-2-methoxy benzhydrazide **5** was treated with acetic anhydride to afford compound **6a**,[34] or, in alternative, with trifluoroacetic anhydride in the presence of triethylamine, to introduce a trifluoroacetate group and yield **6b**. Cleavage of the Boc moiety and coupling of **6a** and **6b** to *N*-Boc-Val-OH afforded the peptidomimetic strands **7a** and **7b,** which, after removal of the Boc protecting group were coupled to either diketopiperazine scaffold *cis*-DKP or *trans*-DKP. This coupling was realized by the use of the triazine-based reagent DMTMM(BF_4),[35] since other activating reagents failed to achieve the coupling or afforded the products in low yield and/or with major impurities. Conversely, through the use of DMTMM(BF_4), compounds **8a-8d** were obtained in satisfactory yields (40-54%). The tetrapeptide sequences Gly-Val-Val-Ile and Lys-Leu-Val-Phe were then constructed in the lower arm in a step by step solution phase synthesis. The *N*-Boc protected amino acids were coupled in good yields using HATU and HOAt in DMF, and the protected modulator precursors **13a**-**13d** were eventually obtained. Final deprotection of the main and side chain protecting groups afforded compounds **1**-**4**. Purification via preparative HPLC and lyophilization gave the pure TFA salts, for the subsequent conformational analysis and aggregation inhibition studies.

The conformation of **1** was recently studied by NMR and the formation of a stable hairpin **1** verified and corroborated by computational studies, which also assessed the safe extrapolation of the structural characteristics found in the NMR studies in methanol to the aqueous environment.[33] The conformation of the derivative **2** was then investigated in methanol (see Figure 2 for the structure of compound **2** and the residue numbering). Attempts to perform these studies in aqueous solutions were hampered by the low solubility of these compounds and the broad line-widths of the resulting spectra.

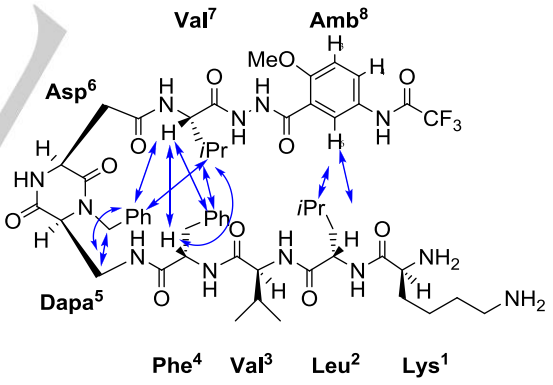

Figure 2. Structure of hairpin mimic **2** highlighting the residue numbering and the most important interstrand ROEs. Residue abbreviations: Dapa, 2,3-diaminopropionic acid; Amb, 5-amino-2-methoxy benzhydrazide unit

The $^1H\alpha$ and $^{13}C\alpha$ chemical shift deviations (CSD, defined as the differences between experimental chemical shifts and corresponding random coil values) of Leu^2, Val^3, Phe^4 and Val^7 residues proved that extended conformations of amino acids predominate (see supporting information, Table S3), as supported by upfield shifted Cα carbons (negative CSD values between –4.6 and –1.9 ppm), and downfield shifted Hα protons (positive CSD values > 0.1 ppm). The large vicinal $^3J_{HN\text{-}H\alpha}$ coupling constants (7.8–9.7 Hz) also reflected ϕ dihedral angles corresponding to β conformations.

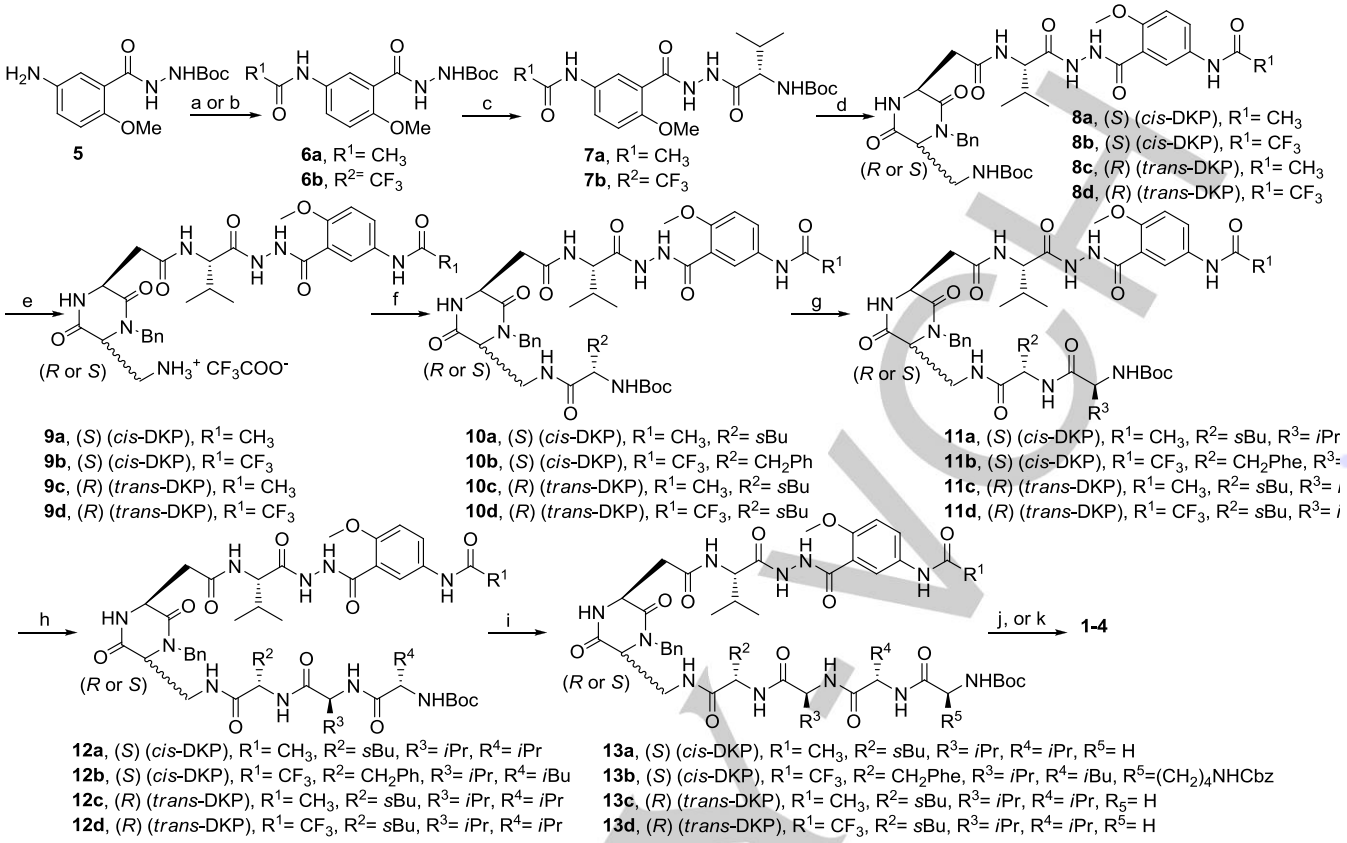

Scheme 1. ***a)*** Ac_2O, THF, quantitative yield; ***b)*** $(CF_3CO)_2O$, TEA, THF, 89%; ***c)*** 1) TFA, CH_2Cl_2, quantitative yield; 2) Boc-Val-OH, HBTU, HOBt, DIPEA, DMF, overnight, 69% (**7a**), 80% (**7b**); ***d)*** 1) TFA, CH_2Cl_2, quantitative yield, 2) H_2N-DKP-$COOCH_2CH{=}CH_2$ DMTMM(BF_4), NMM, DMF, overnight, 0 °C to r.t., 45% (**8a**), 40% (**8b**), 54% (**8c**), 52% (**8d**); ***e)*** TFA, CH_2Cl_2, quantitative yield, ***f)*** HATU, HOAt, DIPEA, Boc-Ile-OH or Boc-Phe-OH, DMF, 0 °C to r.t., overnight, 78% (**10a**), 87% (**10b**), 98% (**10c**), 98% (**10d**); ***g)*** 1) TFA, CH_2Cl_2, quantitative yield, 2) HATU, HOAt, DIPEA, Boc-Val-OH, DMF, 0 °C to r.t., overnight, 83% (**11a**), 76% (**11b**), 80% (**11c**), 85% (**11d**); ***h)*** 1) TFA, CH_2Cl_2, quantitative yield, 2) HATU, HOAt, DIPEA, Boc-Val-OH or Boc-Leu-OH, DMF, 0 °C to r.t., overnight, 74% (**12a**), 75% (**12b**), 60% (**12c**), 90% (**12d**); ***i)*** 1) TFA, CH_2Cl_2, quantitative yield, 2) HATU, HOAt, DIPEA, Boc-Gly-OH or Boc-Lys(Cbz)-OH, DMF, 0 °C to r.t., overnight, 77% (**13a**), 75% (**13b**), 67% (**13c**), 65% (**13d**); j) TFA, CH_2Cl_2, overnight, quantitative yield, **1**, **3**, **4**; k) Pd/C, H_2, MeOH, then TFA, CH_2Cl_2, overnight, quantitative yield **2**.

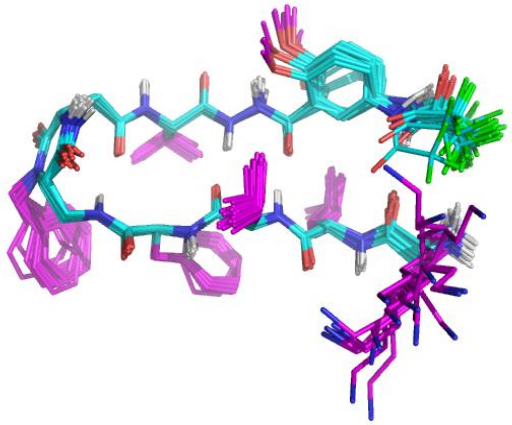

Figure 3. Structure of **2** calculated using NMR conformational parameters observed in methanol. The 20 conformers were superimposed by best fitting of backbone heavy atoms. Fluorine, nitrogen, oxygen, backbone and side-chain carbon atoms are coloured in green, blue, red, cyan and magenta, respectively. HN hydrogen atoms are shown in grey. The figure was prepared with PyMOL.

Finally, the analysis of Hα-HN ROE correlations showed strong sequential and medium intra-residual Hα-HN ROEs, which are characteristic of extended backbone conformations. The most compelling evidence for the formation of a β-hairpin came from the observation of numerous ROEs between the two arms. Indeed, 14 interstrand ROEs could be detected, involving backbone and side-chain protons of Val[7] with Phe[4]-Dapa[5], and Amb[8] H6 proton with Leu[2]-Val[3] protons (see Figure 2 for residue numbering and the most important interstrand ROEs and supporting information, Figure S1, Table S5). The NMR structures of **2** were then calculated by restrained molecular dynamics based on distance and dihedral angle restraints inferred from NMR data (see supporting information, Table S5). Structures adopt a well-defined β-hairpin conformation (Figure 3), with the formation of 3 to 4 inter-strand hydrogen bonds. The conformers show fraying at the extremities of both arms, the hydrogen bond between Lys[1] and the terminal acetamido group being not systematically observed. Dapa[5] amide proton exhibits

a small negative temperature coefficient ($\Delta\delta$HN/ΔT value of –4.3 ppb/K, see supporting information, Table S3), in agreement with its involvement in a hydrogen bond. Other amide protons show larger variations, which may be ascribed to an increased flexibility of the β-sheet toward the extremities. The structures are further stabilized by van der Waals interactions between Leu[2], Phe[4] and Val[7] residues and the DKP-*N*-benzylic group, forming a large hydrophobic face. The NMR conformers show well-defined side-chain conformations, χ1 rotamers being *gauche*– (~ –60°) for Leu[2] and Phe[4], *trans* (~180°) for Val[7] and *gauche*+ (~ +60°) for Val[3].

We next examined the conformational preferences of the *trans*-DKP derivative **4**. The Val[2,3,7] and Ile[4] residues tended to adopt extended backbone conformations, as indicated by upfield shifted Cα carbons (negative CSD values between –3.5 and –1.7 ppm), and downfield shifted Hα protons (positive CSD values, excepted Ile[4], see supporting information, Table S4). These extended conformations were further supported by the large $^3J_{HN\text{-}H\alpha}$ coupling constants (> 8 Hz) and the analysis of 2D ROESY spectrum revealing strong sequential and medium intraresidual Hα-HN correlations. However, no long-range ROEs could be detected between the two arms, proving that **4** did not adopt an intramolecular β-hairpin conformation. The amide protons also showed a large variation of their chemical shift with temperature ($\Delta\delta$HN/ΔT between –9 and –6 ppb/K) confirming that they were not involved in intramolecular hydrogen bonds (see supporting information, Table S4). Notably, significant chemical shift changes were observed on 1D ^{1}H spectra upon concentration variation (10 μM – 0.4 mM) suggesting that **4** could be prone to association through intermolecular hydrogen bonding.

ECD spectra were also measured for compounds **2** and **4** (0.1 mM in methanol, see Figure S2 in the Supporting Information). The two curves display similar features, which can hardly be traced back to any of the canonical secondary structures of peptides. This can probably be ascribed to the presence of the the 5-amino-2-methoxybenzhydrazide chromophore contributing to the observed CD signal in the far UV region.

In summary, peptidomimetics containing the *cis*-DKP scaffold can exist in β-hairpin conformation and, as such can be expected to act as β-sheet binders and $A\beta_{1\text{-}42}$ aggregation inhibitors. On the contrary, peptidomimetics containing the *trans*-DKP are unable to form β-hairpin structures although the two arms adopt extended conformations which, in principle, could still actively interact with $A\beta_{1\text{-}42}$ amyloid peptide.

Modulation of amyloid aggregation by peptidomimetics 1-4

Thioflavin T fluorescence assays are a benchmark methodology to monitor the kinetics of aggregation of amyloid proteins [36] and their modulation by amyloid β-sheet mimics.[26, 27, 28, 29] The ability of compounds **1**-**4** and of a few of their synthetic precursors or fragments to interfere with the *in vitro* $A\beta_{1\text{-}42}$ fibrillization process, was thus investigated. The fluorescence curve for $A\beta_{1\text{-}42}$ alone at a concentration of 10 μM followed the typical sigmoid pattern with a lag phase (between 4 to 10 h, depending on the experiment), an elongation phase and a final plateau reached after 12 to 20 h. Two parameters were derived from the ThT curves: $t_{1/2}$, defined as the time at which the half maximal ThT fluorescence is reached, is a measure of the aggregation process rate; and *F*, the fluorescence value of the final plateau which is assumed to be dependent on the amount of fibrillar material formed (Table 1). On the contrary, no fluorescence was observed, up to the maximum 100 μM concentration used in this assay, in the solutions containing compounds **1-4** alone, presuming that no extensive self-aggregation occured. The activity of β-hairpin **1** based on the *cis*-DKP and bearing the peptidic sequence GVVI and the peptidomimetic 5-acetamido-2-methoxy benzhydrazide was then investigated. A modest inhibitory effect on $A\beta_{1\text{-}42}$ fibrillization was observed, albeit at the high **1**/$A\beta_{1\text{-}42}$ ratio of 10/1 (Table 1). At this ratio, **1** delayed the rate of aggregation of $A\beta_{1\text{-}42}$ ($t_{1/2}$ was increased by almost a factor 2, 186 %) and slightly decreased the fluorescence plateau (equal to 71 % of F of the control experiment).

Table 1. Effects of compounds **1-4** on $A\beta_{1\text{-}42}$ fibrillization assessed by ThT-fluorescence spectroscopy at compound/Aβ ratios of 10/1 and 1/1).

Compound	Compound/ $A\beta_{1\text{-}42}$ / ratio [a]	$t_{1/2}$ variation factor (%) [b]	F variation factor (%) [b]
1	10 / 1 1 / 1	186±22 % ne	71±3 % ne
2	10 / 1 1 / 1	NA 222±36 %	3±2 % 29±2 %
3	10 / 1 1 / 1	160±12 % ne	72±18 % ne
4	10 / 1 1 / 1	23±4 % ne	67±4 % ne

ne = no effect, NA = no aggregation. Variation factors are expressed as mean ± SE, n=3-6. [a] The concentration of $A\beta_{1\text{-}42}$ in this assay is 10 μM. [b] See supporting information for the calculation of the $t_{1/2}$ and *F* variation factors (<100% means a decrease, >100% means an increase).

Peptidomimetic **3**, containing the *trans*-DKP scaffold and the same two arms as **1**, was then studied. Also in this case, a minimal delay in the aggregation process (even lower than **1,** 160 *vs* 186 % of the $t_{1/2}$ of the control) was observed with almost no effect on the intensity of the fluorescence plateau. In order to evaluate the role of the two arms, the tetrapeptide sequence GVVI-NH_2 (primary amide at the C-terminus), and the deprotected peptidomimetic arm **7a** (after TFA cleavage of the Boc protecting group), were tested. A modest acceleration in the aggregation rate and a more pronounced increase of the fluorescence plateau were observed with the tetrapeptide sequence, whereas the deprotected peptidomimetic arm showed no activity (see supporting information Table S6). In order to study the effect of introducing a hydrophobic trifluoromethyl group versus a methyl group, the acetyl capping group at the 5-amino-2-methoxybenzhydrazide unit (R_1 = CH_3, compound **3** in Figure 1) was replaced by a trifluoroacetyl group (R_1 = CF_3, compound **4** in Figure 1). Interestingly, the activity was significantly affected. Compound **4** (Table 1 and supporting information Figure S3) promoted the aggregation of $A\beta_{1\text{-}42}$ at a 10/1 ratio, with a significant reduction of $t_{1/2}$ (equal to only 23% of $t_{1/2}$ of the control). In addition, the final fluorescence intensity was also slightly decreased (equal to only 67% of *F* of the control) indicating that the amount and/or morphology of the fibers might be different from those of the control sample. The beneficial effect of triflluoromethylation of the 5-amino-2-methoxybenzhydrazide unit was further corroborated by the observation that compounds **9b** (*cis*-DKP) and **9d** (*trans*-DKP), i.e. the synthetic intermediates containing the DKP scaffolds and

the peptidomimetic arm, displayed a significant activity on the aggregation process while **9a** and **9c** (their methylated analogs) had no effect. In fact, the *cis* analog **9b** slightly accelerated the aggregation while the *trans* analog **9d** significantly delayed it even at the low 1/1 **9d**/A$\beta_{1\text{-}42}$ ratio (see supporting information Table S6 and Figure S3). Analyzing these first results, compounds **1**, **3** and **4**, containing the GVVI tetrapeptide sequence, behave as modest modulators of the aggregation of A$\beta_{1\text{-}42}$ at the high 10/1 compound/A$\beta_{1\text{-}42}$ ratio, while they displayed no activity at the stoichiometric 1/1 ratio.

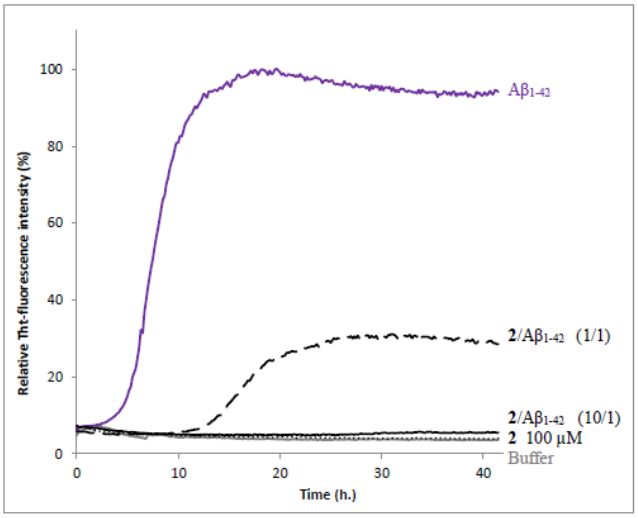

Figure 4. Representative curves of ThT fluorescence assays over time showing A$\beta_{1\text{-}42}$ (10 µM) aggregation in the absence (purple curves) and in the presence of compounds **2** (black curves) at compound/A$\beta_{1\text{-}42}$ ratios of 10/1 and 1/1.

For this reason, we decided to investigate the KLVF tetrapeptide sequence, alone or inserted in peptidomimetic derivatives. The tetrapeptide KLVF-NH_2 very slightly delayed the aggregation ($t_{1/2}$ was increased by 38%, see supporting information) at the ratio of 10/1 (KLVF/A$\beta_{1\text{-}42}$), although it had no significant effect on the fluorescence plateau. This result indicates that the sequence KLVF might be more favorable to decrease the aggregation process than GVVI which is more likely to accelerate it. Indeed, hairpin **2** (Figure 1), where the KLVF tetrapeptide was linked to the *cis*-DKP scaffold and to the 5-trifluoroacetamido-2-methoxybenzhydrazide peptidomimetic arm completely suppressed the ThT fluorescence at a **2**/A$\beta_{1\text{-}42}$ ratio of 10/1 (See Table 1 and Figure 4) indicating or a total inhibition of A$\beta_{1\text{-}42}$ fibrillization or a different pathway of aggregation conducting to aggregates with different morphology than the one of classical fibers and that do not bind ThT. Hairpin **2** still displayed a very good efficiency at a stoichiometric ratio ($t_{1/2}$ was more than doubled, 222% and the final fluorescence intensity was only of 29% of the control value, see Table 1 and Figure 4). This result confirms that the *cis* configuration of the DKP scaffold combined with the tetrapeptide KLVF and the trifluoroacetamido-2-methoxybenzhydrazide-based peptidomimetic are beneficial for the modulation of A$\beta_{1\text{-}42}$ fibrillization. The Boc-protected compounds **13a**-**13d**, precursors of the final compounds **1**-**4** were also evaluated. However, they all tended to self-aggregate (at 100 µM and even slightly at 10 µM) and to be self-organized in structures that bind the ThT dye already in the control experiments (see supporting information Table S6), preventing their evaluation.

Summarizing, among the four peptidomimetics prepared, **2** and **4** showed interesting properties in modulating A$\beta_{1\text{-}42}$ aggregation process, where compound **2** inhibited the aggregation, while compound **4** accelerated it. For this reason, we decided to investigate in more detail their mechanism of aggregation modulation.

It is well known that the Tht- binding assays present limitations and drawbacks in the evaluation of amyloid aggregation: Indeed, some small aromatic compounds were observed to displace the thioflavin from its binding site into the amyloid beta-sheet, decreasing the fluorescence signal, and thus producing false positives.[37] A deeper insight in the extent and pathways of Aβ aggregation can be obtained by a combination of different methodologies and in particular of capillary electrophoresis (CE) and transmission electron microscopy (TEM).

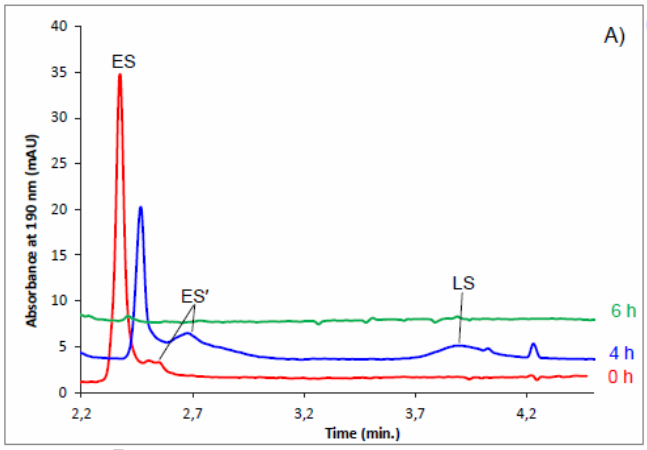

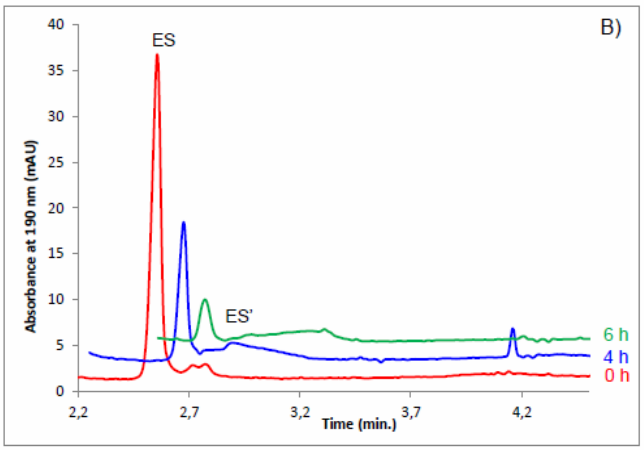

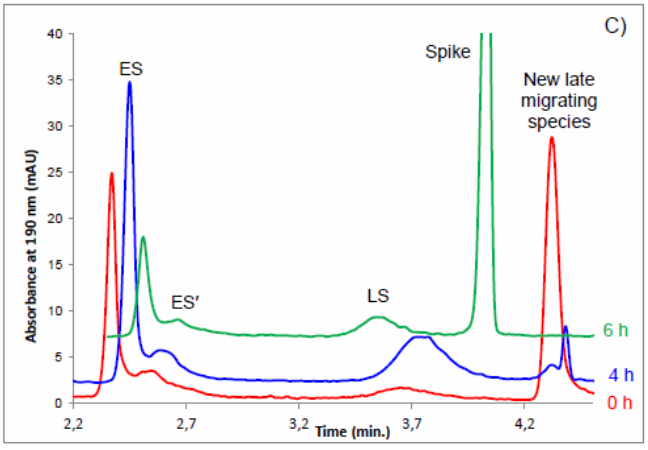

Figure 5. Electrophoretic profile obtained immediately (0 h), 4 h and 6 h after sample reconstitution (t_0) of $A\beta_{1-42}$ peptide (100 µM) alone (A), in the presence of compound **2** at **2**/$A\beta_{1-42}$ ratio of 1/1 (B) and in the presence of compound **4** at **4**/$A\beta_{1-42}$ ratio of 1/1 (C).

Specifically, while transmission electron microscopy (TEM) analyses have been used to reveal the formation and morphology of higher molecular weight and insoluble Aβ aggregates, we have recently reported a CE method to monitor the early steps of the oligomerization process over time, and in particular the formation of small soluble oligomers.[38] This technique allows the evaluation of the impact of small molecules on three key species, (i) the monomer of $A\beta_{1-42}$ (peak ES), (ii) different small metastable oligomers grouped under peak ES' and (iii) transient later species corresponding to oligomers larger than dodecamers (peak LS).[38, 39] Aggregation kinetics of $A\beta_{1-42}$ alone showed that overtime, the peak of monomer ES decreased in favor of the peaks of oligomers ES' and LS, and that soluble species were no longer visible after 6 h (Figure 5A). The electrophoretic profiles obtained in the presence of the *cis*-DKP derivative **2** indicated that **2** delayed the aggregation process and maintained the presence of the monomer ES which was still present after 6 h (Figure 5B). Small and large oligomeric species were only slightly visible after 4 and 6 h. These results suggest that **2** prevents small oligomeric species to be formed even at the **2**/$A\beta_{1-42}$ ratio of 1/1 small oligomeric species being considered as mainly responsible for the neurotoxicity associated with AD.[3,4,14-15,17] The electrophoretic profiles obtained in the presence of the *trans*-DKP derivative **4** (Figure 5C) indicated that **4** modulated the oligomerization process. Indeed, as early as the beginning of the kinetics (t_0), the CE profile of the sample containing **4** exhibited already the presence of ES together with several oligomeric species as ES´ and LS and with new late migrating species. The most remarkable one is the new later species observed after 4.2 min, which did not appear in the control profile. Interestingly, the ES peak (monomer form) started to decrease only after the period of 6 h and therefore late compared to the control. The overall results indicate that compound **4** accelerates the oligomerization process but probably through a different pathway than the one observed for $A\beta_{1-42}$ alone.

TEM analyses were performed on compounds **2** and **4** under the same conditions employed for the ThT studies. For compound **2**, images were recorded after 42 h of preincubation with the peptide, corresponding to the end of the ThT-fluorescence kinetics (Figure 6). A typical and very dense network of fibers was observed in the $A\beta_{1-42}$ control sample (Figure 6, left image). On the grid containing $A\beta_{1-42}$ incubated with compound **2** at a **2/**$A\beta_{1-42}$ ratio of 10/1 (Figure 6, middle image), the network was substantially less dense with the presence of globular aggregates rather than mature fibrils observed in the control sample. This globular morphology was also observed in the sample containing $A\beta_{1-42}$ incubated with compound **2** at a stoichiometric ratio (Figure 6, right image), where the network was also less dense than in the control sample. This is in accordance with the ThT assays where **2** was shown to totally inhibit the ThT fluorescence at a **2/**$A\beta_{1-42}$ ratio of 10/1 and still decrease the final fluorescence plateau at a **2/**$A\beta_{1-42}$ ratio of 1/1. As the CE analysis showed a decrease of the early oligomerization process, and as both ThT and TEM experiments showed a decrease of the fibrillization process, the combination of the three methods indicate that **2** is able to decrease the overall kinetics of aggregation and to change the pathway of fibrillization forming more globular aggregates.

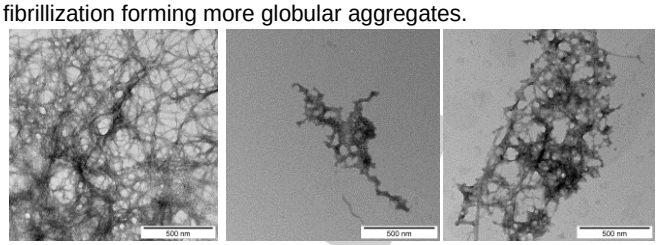

Figure 6. Effects of the hairpin **2** on $A\beta_{1-42}$ fibril formation visualized by TEM. Negatively stained images were recorded at 42 h of incubation of $A\beta_{1-42}$ (10 µM in 10 mM Tris.HCl, 100 mM NaCl at pH = 7.4) alone (left row), in the presence of 100 µM (middle row), and 10 µM (right row) of **2**. Scale bars, 500 nm.

Compound **4** was studied at the higher ratio (**4/**$A\beta_{1-42}$ ratio of 10/1) since it displayed no significant effect at the stoichiometric ratio in the ThT experiment. TEM images were recorded at 5 h (during the lag time of $A\beta_{1-42}$ alone) and 29 h (once the fluorescence plateau was reached) of the fibrillization kinetics (see the ThT curves, Figure S3 in supporting informations). Major differences were observed in the morphology and in the quantity of aggregates formed in presence of **4** (Figure 7). After 5 h of aggregation whereas the sample of $A\beta_{1-42}$ alone had almost aggregated into short fibrils, the sample incubated with **4** showed a denser network of fibers which are substantially thicker. At 29 h, once the maximum aggregation was reached, a dense network of fibers with the classical morphology is observed for $A\beta_{1-42}$ alone. A network of comparable density, composed of significantly thicker fibers, was observed in the $A\beta_{1-42}$ sample incubated with **4**. This different morphology might explain the different plateau of fluorescence observed in the ThT assays. We hypothesized that **4** having the propensity to self-associate, as observed by NMR (see above), it could be involved in nucleus formation triggering $A\beta_{1-42}$ oligomerization, as seen in the CE experiments, and accelerating aggregation. Although accelerating the aggregation pathways is less intuitive, this strategy has recently aroused interest [40] and needs further investigations. Indeed, methylene blue (MB), which has reached clinical trials, promotes fibrillization,[40c] and few compounds that accelerate $A\beta_{1-42}$ fibril formation reduce the concentration of soluble $A\beta_{1-42}$ oligomers and demonstrate a reduced toxicity for mammalian cells.[40a-b]

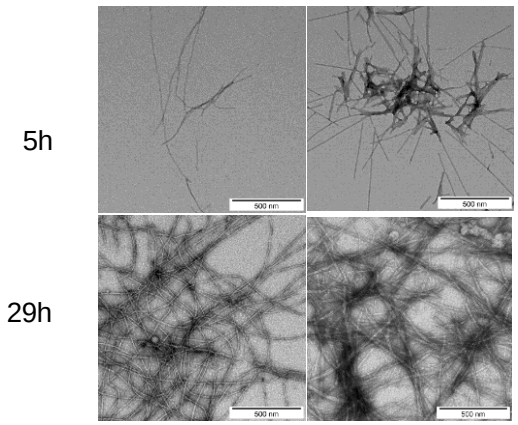

Figure 7. Effects of the hairpin **4** on $A\beta_{1-42}$ fibril formation visualized by TEM. Negatively stained images were recorded at 5 h and 29 h of incubation of $A\beta_{1-42}$ (10 µM in 10 mM Tris.HCl, 100 mM NaCl at pH = 7.4) alone (left row) and in the presence of 100 µM of **4** (right row). Scale bars, 500 nm.

Conclusions

We described the design and the synthesis of four new acyclic peptidomimetics composed of a bifunctional diketopiperazine scaffold DKP, as a potential β-turn inducer, a peptidomimetic arm and a tetrapeptide arm. The compounds containing the *cis*-DKP (namely **1** and **2**) adopted stable β-hairpin mimic conformations, and the present work validates the capacity of small β-hairpin peptidomimetics to interact with $A\beta_{1-42}$ peptide in order to modulate its aggregation. On the other hand, peptidomimetics containing the *trans*-DKP are unable to form β-hairpin structures, although the two arms adopt extended conformations, which could still actively interact with $A\beta_{1-42}$ amyloid peptide. And in fact, compound **4** accelerated the aggregation by promoting the early oligomerization process, albeit probably through a different pathway than the one of $A\beta_{1-42}$ alone. We confirmed that in both *cis* and *trans* series, the whole molecules were essential for the activity, as fragments or truncated compounds displayed no or lower efficacy to modulate $A\beta_{1-42}$ aggregation. We clearly demonstrated that both hydrophobic peptide KLVF and GVVI inspired by the central and *C*-terminal sequence of $A\beta_{1-42}$ respectively, and involved in the β-sheet structuration of $A\beta_{1-42}$ aggregates, were good recognition elements to bind $A\beta_{1-42}$, although, KLVF was shown to be more beneficial for inhibiting the aggregation process. The capacity of the *N*-terminus of peptidomimetics and of the lysine residue to form ionic interactions with acidic residues of $A\beta_{1-42}$ seems an essential criterion for a good activity. In both *cis* and *trans* series, the introduction of a hydrophobic trifluoromethyl group in the peptidomimetic arm increased the affinity for $A\beta_{1-42}$ and thus notably influenced the activity of the molecules. In conclusion, this work demonstrates that compound **2**, a small β-hairpin peptidomimetic is able to modulate and decrease fibrillization and early oligomerization process of $A\beta_{1-42}$,. preventing the formation of small and soluble $A\beta_{1-42}$ oligomers, which are described by several groups as primarily responsible for neurotoxicity. Maintaining an acyclic β-hairpin while decreasing the peptidic character could provide valuable insights to develop druggable β-hairpin mimics as aggregation inhibitors of amyloid-forming proteins.

Experimental Section

Chemistry

Usual solvents were purchased from commercial sources and dried and distilled by standard procedures. The following compounds were prepared according to published methods: *Cis*-DKP,[31] *trans*- DKP,[32b] compounds **6a**-**13a** and **1**.[33] Pure products were obtained after flash chromatography using Merck silica gel 60 (40-63 µm). TLC analyses were performed on silica gel 60 F250 (0.26 mm thickness) plates. The plates were visualized with UV light (λ = 254 nm) or revealed with a 4 % solution of phosphomolybdic acid or ninhydrin in EtOH. Elemental analyses (C, H, N) were performed on a Perkin-Elmer CHN Analyser 2400 at the Microanalyses Service of the Faculty of Pharmacy in Châtenay-Malabry (France). HRMS were obtained using a TOF LCT Premier apparatus (Waters), with an electrospray ionization source. NMR spectra were recorded on an ultrafield AVANCE 300 (^{1}H, 300 MHz, ^{13}C, 75 MHz) or a Bruker 400 (^{1}H, 400 MHz, ^{13}C, 100 MHz, ^{19}F 376 MHz). Chemical shift δ are in parts per million (ppm) and the following abbreviations are used: singlet (s), doublet (d), doublet of doublet (dd), triplet (t), multiplet (m), and broad singlet (bs). Melting points were determined on Kofler melting point apparatus and are uncorrected.

General procedures

General procedure A for deprotection reactions: To a solution of the *N*-Boc-protected amino acid or peptide in CH_2Cl_2 (0.13 M) was added a half volume of TFA and the reaction was stirred at r.t. for 1-3 h. The solvent was evaporated, toluene (2×) was added followed by evaporation, and then ether was added and evaporated to afford the corresponding TFA salt.

General procedure B for coupling reactions: The *N*-protected amino or peptide acid (3 equiv) was dissolved in DMF (0.1 M) under the nitrogen atmosphere and the solution was cooled in an ice bath, followed by adding HOAt (3 equiv), HATU (3 equiv) and DIPEA (5 equiv). The solution was stirred at 0 °C for 1 h and then was added the solution of TFA salt in DMF. The reaction was stirred at 0 ºC for 30 minutes to 1 h and at r.t. overnight. The DMF was evaporated and the mixture was diluted with EtOAc and consecutively extracted with 1 M $KHSO_4$ (2×) or citric acid (10% solution), aqueous $NaHCO_3$ (2×) and brine (1×), dried over Na_2SO_4 and the solvent evaporated under reduced pressure to afford the crude product.

General procedure C for coupling reactions: To a solution of the *N*-protected amino acid in DMF (0.1 M), under nitrogen atmosphere and at 0 ºC, was added DMTMM (BF_4) (1equiv) and NMM (3 equiv). After 30 min, a solution of the TFA salt of the peptide in DMF was added and the reaction mixture was stirred at 0 ºC for 1 h and at r.t. overnight. The solvent was evaporated and the residue was diluted with EtOAc and consecutively extracted with 1 M $KHSO_4$ (2×) or citric acid (10% solution), aqueous $NaHCO_3$ (2×) and brine (1×), dried over Na_2SO_4 and the solvent evaporated under reduced pressure to afford the crude product.

Synthesis of 2

To a solution of **13b** (59 mg, 0.043 mmol) in 3 mL MeOH was added Pd/C (6 mg, 10% weight). The reaction flask was flushed three times with hydrogen, and the reaction was stirred, under hydrogen atmosphere, for 1 h at r.t. The mixture was filtered through an HPLC filter, then the filtrated solution was evaporated under reduced pressure to afford product without Cbz protecting group that undergoes the deprotection reaction according to general procedure A. The reaction is left overnight under stirring to obtain product **2** as a light pink solid (60mg, quantitative yield over two steps). ^{1}H NMR (400 MHz, DMSO) δ 11.33 (s, NH, 1H), 10.46 (s, NH, 1H), 10.13 (s, NH, 1H), 8.51 (d, *J*= 4 Hz, 1H), 8.38-8.35 (m, 3H), 8.21-8.09 (m, 7H), 7.97 (d, *J*= 4 Hz, 2H), 7.85-7.79 (m, 4H), 7.34-7.14 (m, 15H), 5.03 (d, *J*= 16 Hz, 1H), 4.72 (m, 1H), 4.49 (t, *J*= 8 Hz, 1H), 4.42 (m, 1H), 4.31 (m, 1H), 4.18 (t, *J*= 8 Hz, 1H), 4.09 (d, *J*= 16 Hz, 1H), 3.90 (s, 3H), 3.83-3.79 (m, 2H), 3.66-3.56 (m, 2H), 2.93-2.73 (m, 7H), 2.02 (m, 1H), 1.91 (m, 1H), 1.70-1.67 (m, 2H), 1.59-1.52 (m, 4H), 1.44-1.34 (m, 5H), 1.28-1.23 (m, 4H), 0.98-0.93 (m, 6H), 0.87-0.74 (m, 12H); ^{13}C NMR (100 MHz, DMSO) δ 171.6, 171.4, 171.0, 170.9, 169.3, 169.0, 168.4, 168.3, 166.2, 165.3, 162.9,

158.8, 158.5, 154.7, 154.6, 137.5, 136.7, 129.4, 129.2, 129.0, 128.6, 128.3, 128.1, 127.9, 127.4, 126.3, 125.7, 125.4, 123.6, 121.5, 112.8, 62.2, 62.1, 58.3, 57.8, 56.3, 53.6, 53.5, 51.9, 51.7, 51.3, 48.0, 46.8, 41.9, 40.6, 40.4, 39.2, 38.5, 38.4, 37.9, 32.5, 31.0, 30.7, 30.6, 29.4, 26.5, 24.1, 23.1, 21.5, 21.0, 19.2, 19.1, 18.5, 18.1, 16.7, 12.4; ^{19}F NMR (188 MHz, *d6*-DMSO) δ = −73.92 (s, 6F, CF_3COOH); -74.26 (s, 3F, CF_3CO) ; HRMS Calc for $C_{55}H_{75}F_3N_{12}O_{11}$ $[M+H]^+$ (1137.5630): found 1137.5709; IR ν_{max}: 3280, 2975, 1688, 1647, 1497, 1202, 1163.

Synthesis of 3

Compound **13c** (0.014 mmol, 1 equiv) was deprotected according to general procedure A affording compound **3** (14 mg, 92%) as a light yellow solid. mp: 186-190 °C; ^{1}H NMR (400 MHz, DMSO) δ 9.94 (d, *J*= 8 Hz, NH, 1H), 8.38 (d, *J*= 8 Hz, NH, 1H), 8.24 (t, *J*= 4 Hz, NH, 1H), 8.12-8.06 (m, NH, 3H), 7.96 (d, *J*= 4 Hz, 1H), 7.77 (dd, *J*= 8, 20 Hz, 2H), 7.34-7.26 (m, 5H), 7.11 (d, *J*= 8 Hz, 1H), 5.28 (d, *J*= 16 Hz, 1H), 4.39-4.33 (m, 3H), 4.23-4.15 (m, 2H), 4.00 (d, *J*= 16 Hz, 1H), 3.86 (s, 3H), 3.68-3.61 (m, 3H), 3.52 (m, 1H), 2.87-2.78 (m, 2H), 2.02 (s, 3H), 1.98-1.91 (m, 2H), 1.68 (m, 1H), 1.38 (m, 1H), 0.96-0.91 (m, 6H), 0.87-0.76 (m, 18H); ^{13}C NMR (101 MHz, DMSO) δ 171.8, 170.7, 170.4, 169.3, 169.2, 168.1, 166.6, 165.9, 165.7, 163.4, 152.7, 132.6, 128.4, 127.9, 127.3, 123.4, 123.1, 121.4, 112.5, 66.0, 58.6, 58.1, 57.4, 56.6, 56.2, 56.0, 50.4, 46.4, 40.1, 38.8, 36.5, 34.1, 30.9, 30.1, 24.1, 23.8, 19.3, 19.2, 19.1, 18.5, 18.2, 17.9, 15.2, 10.7; HRMS Calcd for $C_{47}H_{70}N_{11}O_{11}^+$ [M (NH_3^+)] (964.5251): found 964.5274; IR ν_{max}: 3279, 2966, 2359, 1634, 1541, 1497, 1470, 1152.

Synthesis of 4

Compound **13d** (0.019 mmol, 1 equiv) was deprotected according to general procedure A affording compound **4** (20 mg, 92%) as a yellow solid. mp: 216-220 °C; ^{1}H NMR (400MHz, DMSO) δ 11.32 (s, NH, 1H), 10.31 (s, NH, 1H), 9.97 (s, NH, 1H), 8.40 (d, *J*= 8 Hz, NH, 1H), 8.25 (t, *J*= 4 Hz, 1H), 8.11 (d, *J*= 8 Hz, 1H), 8.07 (m, 5H), 7.81-7.79 (m, 2H), 7.33-7.27 (m, 5H), 7.22 (d, *J*= 8 Hz, 1H), 5.28 (d, *J*= 16 Hz, 1H), 4.41-4.34 (m, 3H), 4.23-4.15 (m, 2H), 4.00 (d, *J*= 16 Hz, 1H), 3.89 (s, 3H), 3.54 (m, 2H), 2.89-2.73 (m, 2H), 2.06-1.95 (m, 3H), 1.68 (m, 1H), 1.41 (m, 1H), 1.28-1.23 (m, 2H), 1.09 (m, 1H), 0.97-0.91 (m, 6H), 0.87-0.76 (m, 18H); ^{13}C NMR (101 MHz, DMSO) δ 171.9, 170.7, 170.5, 169.4, 169.3, 166.6, 165.9, 165.7, 163.1, 158.4, 154.5, 136.5, 129.3, 128.5, 127.9, 127.3, 125.5, 123.4, 121.7, 114.4, 112.7, 58.6, 58.1, 57.5, 56.7, 56.3, 56.1, 53.6, 50.4, 46.4, 40.1, 38.9, 36.5, 36.4, 31.0, 30.9, 30.1, 24.1, 19.3, 19.2, 19.1, 18.5, 18.2, 17.9, 15.2, 10.7; ^{19}F NMR (376.3 MHz, CD_3OD) δ −74.51 (s, 3F), -74.56 (s, 3F) ;HRMS Calc for $C_{47}H_{67}F_3N_{11}O_{11}^+$ [M (NH_3^+)] (1018.4968): found 1018.5098; IR ν_{max}: 3292, 2967, 2360, 2341, 1647, 1541, 776, 652.

NMR Spectroscopy

Lyophilized compounds **2** and **4** were dissolved at 0.5 mM concentration in 550 µL of CD_3OH (Eurisotop, Saint-Aubin, France). NMR experiments were recorded on a Bruker Avance III 500 MHz spectrometer equipped with a TCI ^{1}H/^{13}C/^{15}N cryoprobe. NMR spectra were processed with TopSpin 2.0 software (Bruker) and analysed with Sparky program (http://www.cgl.ucsf.edu/home/sparky/). ^{1}H and ^{13}C resonances were assigned using 1D ^{1}H WATERGATE, 2D ^{1}H-^{1}H TOCSY (MLEV17 isotropic scheme of 66 ms duration), 2D ^{1}H-^{1}H ROESY (300 ms mixing time), 2D ^{1}H-^{13}C HSQC and 2D ^{1}H-^{13}C HMBC spectra. ^{1}H and ^{13}C chemical shifts were calibrated using the solvent residual peak (CHD_2OH, δ ^{1}H 3.31 ppm, δ ^{13}C 49.5 ppm). The chemical shift deviations were calculated as the differences between observed chemical shifts and random coil values reported in water.[41] The temperature gradients of the amide proton chemical shifts were derived from 1D ^{1}H WATERGATE spectra recorded over a 25°C interval. $^3J_{HN\text{-}H\alpha}$ coupling constants were measured on 1D ^{1}H WATERGATE or 1D ^{1}H selective TOCSY spectra.

NMR structure calculation

Inter-proton distance restraints were derived from ROESY cross-peak volumes integrated using Sparky. Upper bounds for proton pairs were calculated using the isolated spin pair approximation with an additional 20% tolerance. Upper bounds involving equivalent methyl or aromatic protons were set to 3.5, 4.0 or 5.0 Å for strong, medium and weak ROE cross-peak intensities, respectively. The lower bounds were set to the sum of van der Waals radii of protons. Phi angle restraints were derived from $^3J_{HN\text{-}H\alpha}$ coupling constants using a Karplus relationship. Structures were calculated using Amber 14 program.[42] Amino acid residues were built using ff99SB force field. The 5-trifluoroacetamido-2-methoxybenzhydrazide unit was parameterized using gaff force field atom types and partial charges were computed via the AM1-BCC method implemented within Antechamber. Improper angles were added to maintain the planarity around the hydrazide *N–N* bond and the phenyl-acetamido moiety, (n order to facilitate this parametrization task, conformational preference and rotation barriers of a minimal structure containing the Hao unit were studied by performing a DFT potential energy surface scan, see supporting information). A set of 50 structures was calculated by simulated annealing at 1000 K in vacuo using 43 NMR experimental restraints (40 distances and 4 ϕ angles, listed in table S5), and 7 dihedral angle restraints to fix the *trans* or *cis* configuration of amide bonds. Structures were then refined in implicit aqueous solvent using GBSA (Generalized Born Surface Area) model. The refinement protocol consisted of 60 ps restrained molecular dynamics at 300 K followed by energy minimization. The best 20 structures exhibiting the lowest potential energy and no restraint violation (< 0.1 Å and < 5° for distances and dihedral angles restraints, respectively) were selected to represent the final NMR family.

Thioflavin T assay

Thioflavin T was obtained from Sigma. $A\beta_{1\text{-}42}$ was purchased from American Peptide. The peptide was dissolved in an aqueous 1% ammonia solution to a concentration of 1 mM and then, just prior to use, was diluted to 0.2 mM with 10 mM Tris-HCl, 100 mM NaCl buffer (pH 7.4). Stock solutions of tested compounds were dissolved in DMSO with the final concentration kept constant at 0.5% (v/v) (1µL of DMSO in 200 µL). Thioflavin T fluorescence was measure to evaluate the development of $A\beta_{1\text{-}42}$ fibrils over time using a fluorescence plate reader (Fluostar Optima, BMG labtech) with standard 96-wells black microtiter plates. Experiments were started by adding the peptide (final $A\beta_{1\text{-}42}$ concentration equal to 10 µM) into a mixture containing 40 µM Thioflavin T in 10 mM Tris-HCl, 100 mM NaCl buffer (pH 7.4) with and without the tested compounds at different concentrations (100 and 10 µM) at room temperature. The ThT fluorescence intensity of each sample (performed in

duplicate or triplicate) was recorded with 440/485 nm excitation/emission filters set for 42 hours performing a double orbital shaking of 10 s. before the first cycle. The fluorescence assays were performed between 2 and 3 times over different days. The ability of hairpin compounds to modulate $A\beta_{1-42}$ aggregation was assessed considering both the time of the half-life of aggregation ($t_{1/2}$) and the intensity of the experimental fluorescence plateau (F). See supporting information for the calculation of the $t_{1/2}$ and F variation factors.

Transmission electron microscopy

Samples were prepared under the same conditions as in the ThT-fluorescence assay. Aliquots of $A\beta_{1-42}$ (10 µM in 10 mM Tris-HCl, 100 mM NaCl buffer (pH 7.4) in the presence and absence of the tested compounds were adsorbed onto 300-mesh carbon grids for 2 min, washed and dried. The samples were negatively stained for 45 s. on 2 % uranyl acetate in water. After draining off the excess of staining solution and drying, images were obtained using a ZEISS 912 Omega electron microscope operating at an accelerating voltage of 80 kV.

Capillary electrophoresis

Sample preparation: The commercial $A\beta_{1-42}$ was dissolved upon reception in 0.16% NH_4OH (at 2 mg/mL) for 10 minutes at 20°C, followed by an immediate lyophilisation and storage at -20°C as pretreatment. CE experiments were carried out with a PA800 ProteomeLab instrument (Beckman Coulter Inc., Brea, CA, USA) equipped with a diode array detector. UV detection was performed at 190 nm. The prepared sample (as previously described) was dissolved in 20 mM phosphate buffer pH 7.4 containing DMSO (control or Stock solutions of glycopeptides dissolved in DMSO) to kept constant the DMSO/ phosphate buffer ratio at 2.5% (v/v) and the final peptide concentration at 100 µM regardless the peptide/compound ratio. For the CE separation of Aβ oligomers, fused silica capillary 80 cm (10.2 cm to the detector) 50 mm I.D. were used. The background electrolyte was a 80 mM phosphate buffer, pH 7.4. The separation was carried out under -30 kV at 20°C. The sample was injected from the outlet by hydrodynamic injection at 3.44 KPa for 10 s. After each run, the capillary was rinsed for 5 min with water, 1 min with SDS 50 mM, 5 min with NaOH 1 M and equilibrated with running buffer for 5 min.

Acknowledgements

We thank Fondazione CARIPLO (Project RE-D DRUG TRAIN 2010-1373: Multidisciplinary approaches in research and development of innovative drugs: project for an international collaborative training network) for a research grant (to U.P.) and a PhD fellowship to L.V. and S.P. We also gratefully acknowledge Ministero dell'Università e della Ricerca for financial support (PRIN project 2010NRREPL).Claire Troufflard and Karine Leblanc (BioCIS, UMR 8076) are thanked for their help with the NMR experiments and HPLC analysis respectively. Géraldine Toutirais (IFR 83, Service de Microscopie Electronique, Université Pierre et Marie Curie, France) is acknowledged for her advice in TEM experiments.The Ministère de l'Enseignement Supérieur et de la Recherche (MESR) is thanked for financial support for DB. The Laboratory BioCIS is a member of the Laboratory of Excellence LERMIT supported by a Grant from ANR (ANR-10-LABX-33).

Keywords: Amyloid β-peptide • Alzheimer's disease • Foldamers • Hairpins • Peptidomimetics

[1] a) D. Eisenberg, M. .Jucker, *Cell*. **2012**; *148*:1188–1203. b) F. Chiti, C. M. Dobson, *Annu. Rev. Biochem*. **2006**, *75*, 333–366; c) A. Aguzzi, T. O'Connor *Rev. Drug Discov*. **2010,** *9*, 237-248.

[2] a) http://www.alz.co.uk/research/world-report; b) L. Mucke, *Nature*, **2009**, *461*, 895-897.

[3] a) M. Goedert, M. G. A. Spillantini, *Science,* **2006**, *314*, 777-780; b) C. Haas, D. J. Selkoe, *Nat. Rev. Mol. Cell Biol.* **2007**, *8*, 101-112.

[4] K. N. Dahlgren, A. M. Manelli, W. Blaine Stine, L. K. Baker, G. A. Krafft, M. J. LaDu, *J. Biol. Chem.,* **2002**, *277,* 32046-32053.

[5] A. Jan, O. Gokce, R. Luthi-Carter H. A. Lashuel, *J Biol. Chem.,* **2008**, *283*, 28176-28189.

[6] S. I. A. Cohen, S. Linse, M. Luheshi, E. Hellstrand, D. A. White, L. Rajah, D. L. Otzen, M. Vendruscolo, C. M. Dobson, and T. P. J. Knowles, *Proc. Natl. Acad. Sci. USA*, **2013**, *110*, 9758-9763.

[7] S. Matsumura, K. Shinoda, M. Yamada, S. Yokojima, M. Inoue et al., *J. Biol. Chem.,* **2011**, *286*, 11555-11562.

[8] J. S. Jeong, A. Ansaloni, R. Mezzenga, H. A. Lashuel, and G. Dietler, *J. Mol. Biol.* **2013**, *425*, 1765-1781.

[9] T. Lührs, C. Ritter, M. Adrian, D. Riek-Loher, B. Bohrmann, H. Döbeli, D. Schubert, R. Riek, *Proc. Natl. Acad. Sci. USA,* **2005**, *102*, 17342-17347.

[10] A. Laganowsky, C. Liu, R. M. Sawaya, J. P. Whitelegge, J. Park, M. Zhao, *Science,* **2012**, *335*, 1228-1231.

[11] L. Yu, R. Edalji, J. E. Harlan, T. F. Holzman, A. Pereda Lopez, B. Labkovsky, H. Hillen, S. Barghorn et al., *Biochemistry,* **2009**, *48*, 1870-1877.

[12] M. Ahmed, J. Davis, D. Aucoin, D. Sato, S. Ahuja, S. Aimoto, J. J. Elliott, W. E. Van Nostrand, S. O. Smith, *Nat. Struct. Mol. Biol.,* **2010**, *17, 5,* 561-567.

[13] M. A. Wälti, J. Orts, B. Vçgeli, S. Campioni, and R. Riek, *ChemBioChem* **2015**, *16*, 659 – 669.

[14] K. Ono, M. M. Condron, D. B. Teplow, *Proc. Natl. Acad. Sci. USA,* **2009**, *106*, 14745-14750.

[15] G. M. Shankar, S. Li, T. H. Mehta, A. Garcia-Munoz, N. E. Shepardson, I. Smith *et al., Nat. Med.,* **2008**, *14 (8),* 837-842.

[16] P. Prangkio, E. C. Yusko, D. Sept, J. Yang, M. Mayer, *PLoS ONE,* **2012**, *7*, e47261.

[17] P. Cizas, R. Budvytyte, R. Morkuniene, R. Moldovan, M. Broccio, M. Lösche, G. Niaura, G. Valincius, V. Borutaite, *Arch. Biochem. Biophys.,* **2010**, *496*, 84–92.

[18] a) J. Mayes, C. Tinker-Mill, O. Kolosov, H. Zhang, B. J. Tabner, D. Allsop, *J Biol Chem.* **2014**, *289*,12052-62; b) S. I. A. Cohen, S. Linse, L. M. Luheshi, E. Hellstrand, D. A. White, L. Rajah, D. E. Otzen, M. Vendruscolo, C. M. Dobson, T. P. J. Knowles. *Proc Natl Acad Sci U S A.* **2013**, *110*, 9758-9763.

[19] T. Härd, C. Lendel, *J. Mol. Biol*., **2012**, *421*, 441-465.

[20] M. Bartolini, and V. Andrisano, *ChemBioChem.*, **2010**, *11*, 1018-1035.

[21] C. I. Stains, K. Mondal, and I. Ghosh, *ChemMedChem.,* **2007**, *2*, 1674-1692.

[22] T. Liu, G. Bitan, *ChemMedChem.,* **2012**, *7*, 359-374.

[23] F. Belluti, A. Rampa, S. Gobbi, and A. Bisi, *Expert Opin. Ther. Patents*, **2013**, *23(5)*, 581-596.

[24] For a review, see a) ref 18; b) T. Takahashi, H. Mihara, *Acc. Chem. Res.,* **2008**, *41*, 1309-1318; c) B. Neddenriep, A. Calciano, D. Conti, E. Sauve, M. Paterson, E. Bruno, and D. A. Moffet, *Open Biotechnol. J.*, **2011**, *5*, 39-46.

[25] J. Luo, and J. P. Abrahams, Chem. Eur. J., **2014**, *20*, 2410 – 2419.

[26] P.-N. Cheng, C. Liu, M. Zhao, D. Eisenberg and J. S. Nowick, *Nat. Chem.*, **2012**, *4*, 927-933.

[27] G. Hopping, J. Kellock, B. Caughey, and V. Daggett, *ACS Med. Chem. Lett.*, **2013**, *4*, 824−828

[28] Y. Hamada, N. Miyamoto, Y Kiso, *Bioorg. Med. Chem. Lett.*, **2015**, *25*, 1572–1576

[29] Y. Murakoshi, T. Takahashi, and H. Mihara, *Chem. Eur. J.*, **2013**, *19*, 4525 – 4531.

[30] S. Pellegrino, N. Tonali, E. Erba, J. Kaffy, M. Taverna, A. Contini, M. Taylor, D. Allsop, M. L. Gelmi, S. Ongeri *Chemical Science*, **2016**, DOI: 10.1039/C6SC03176E..

[31] a) A.S.M. Ressurreição, A Bordessa, M. Civera, L. Belvisi, C. Gennari, U. Piarulli, *J. Org. Chem.* **2008**, *73*, 652-660; b) R. Delatouche, M. Durini, M Civera, L. Belvisi, U. Piarulli, *Tetrahedron Lett.* **2010**, *51*, 4278-4280.

[32] a) A. S. M. Ressurreicao, R. Delatouche, C. Gennari, U. Piarulli, *Eur. J. Org. Chem.* **2011**, 217–228; b) a) A. S. M. Ressurreicao, A. Vidu, M. Civera, L. Belvisi, D. Potenza, L. Manzoni, S. Ongeri, C. Gennari, U. Piarulli, *Chem.-Eur. J.* **2009**, *15*, 12184–12188;; c) M. Marchini, M. Mingozzi, R. Colombo, I. Guzzetti, L. Belvisi, F. Vasile, D. Potenza, U. Piarulli, D. Arosio, C. Gennari, *Chem.-Eur. J.* **2012**, *18*, 6195-6207.

[33] L. Vahdati, R. Fanelli, G. Bernadat, I. Correia, O. Lequin, S. Ongeri, U. Piarulli, *New J. Chem.*, **2015**, *39*, 3250-3258.

[34] L. Bannwarth, A. Kessler, S. Pèthe, B. Collinet, N. Merabet, N. Boggetto, S. Sicsic, M. Reboud-Ravaux, S. Ongeri, *J. Med. Chem.* **2006**, *49*, 4657-4664

[35] a) Z. J. Kaminski, B. Kolesinska J. Kolesińska, G. Sabatino, Mario Chelli, P. Rovero, M. Błaszczyk, M. L. Główka, A. M. Papini *J. Am. Chem. Soc.* **2005**, *127,* 16912-16920. b) K.G. Jastrzabek, R. Subiros-Funosas, F. Albericio, B. Kolesinska, Z. J. Kaminski, *J. Org. Chem.*,**2011**, *76*, 4506-4513.

[36] H. LeVine 3rd, *Methods Enzymol.,* **1999**, *309*, 274-284.

[37] a) S. A. Hudson, H. Ecroyd, T. W. Kee, J. A. Carver *FEBS Journal* **2009**, *276*, 5960–5972; b) D. D. Soto-Ortega, B. P. Murphy, F. J. Gonzalez-Velasquez, K. A. Wilson, F. Xie, Q. Wang, M. A. Moss, *Bioorg. Med. Chem.* **2011**, *19*, 2596–2602.

[38] D. Brinet, J. Kaffy, F. Oukacine, S. Glumm, S. Ongeri, M. Taverna, *Electrophoresis*, **2014**, *35*, 3302–3309.

[39] a) J. Kaffy, D. Brinet, J-L Soulier, L. Khemtémourian, O. Lequin, M. Taverna, B. Crousse, S. Ongeri, *Eur. J. Med. Chem.* **2014,** *86*, 752-758; b) J. Kaffy, D. Brinet, J-L Soulier, I. Correia, N. Tonali, K. F. Fera, Y. Iacone, A. R. F. Hoffmann, L. Khemtémourian, B. Crousse, M. Taylor, D. Allsop, M. Taverna, O. Lequin, S. Ongeri , *J. Med. Chem.* **2016**, *59*, 2025–2040.

[40] (a) T. Liu, G. Bitan, *ChemMedChem.* **2012**, *7* 359-374 ; (b) J. Bieschke, M. Herbst, T. Wiglenda, *Nature Chem. Biol.* **2012**, *8* , 93-101; (c) M. Necula, L. Breydo, S. Milton, K. Rakez, W.E. van der Veer, P. Tone, C.G. Glabe, *Biochemistry*, **2007**, *46* , 8850-8860.

[41] D. S. Wishart; C. G. Bigam; A. Holm; R. S. Hodges; B. D. Sykes, *J. Biomol. NMR*. **1995**, *5*, 67-81.

[42] D.A. Case, J.T. Berryman, R.M. Betz, D.S. Cerutti, T.E. Cheatham, III, T.A. Darden, R.E. Duke, T.J. Giese, H. Gohlke, A.W. Goetz, N. Homeyer, S. Izadi, P. Janowski, J. Kaus, A. Kovalenko, T.S. Lee, S. LeGrand, P. Li, T. Luchko, R. Luo, B. Madej, K.M. Merz, G. Monard, P. Needham, H. Nguyen, H.T. Nguyen, I. Omelyan, A. Onufriev, D.R. Roe, A. Roitberg, R. Salomon-Ferrer, C.L. Simmerling, W. Smith, J. Swails, R.C. Walker, J. Wang, R.M. Wolf, X. Wu, D.M. York and P.A. Kollman (2015), AMBER 2015, University of California, San Francisco.